



Steady-State and Dynamic Performance of a 9 MW Wind Farm Connected to a Distribution

Neelesh Shah

Research Scholar, M.Tech.

Energy Technology

Takshshial Institute of Engineering and Technology

Jabalpur (M.P.), India

Email: neeshshah@gmail.com

Preeti Rajput

Assistant Professor

Department of Electrical and Electronics Engineering

Takshshial Institute of Engineering and Technology

Jabalpur (M.P.), India

Email: preetirajput@takshshila.org

Abstract— In recent years, wind energy has become one of the most important and promising sources of renewable energy, which demands additional transmission capacity and better means of maintaining system reliability. The stator of the generator is directly connected to the grid while the rotor is connected through a back-to-back converter which is dimensioned to stand only a fraction of the generator rated power. The DFIG brings the advantage of utilizing the turns ratio of the machine, so the converter does not need to be rated for the machine's full rated power.

Keywords:—Doubly Fed Induction Generator, Dynamic simulation of DFIG, Back to Back AC/DC/AC Converter modeling.

1. INTRODUCTION

The additional freedom of reactive power generation by the GSC is usually not used due to the fact that it is more preferable to do so using the RSC. However, within the available current capacity the GSC can be controlled to participate in reactive power generation in steady state as well as during low voltage periods. The GSC can supply the required reactive current very quickly while the RSC passes the current through the machine resulting in a delay. Both converters can be temporarily overloaded, so the DFIG is able to provide a considerable contribution to

grid voltage support during short circuit periods. This report deals with the introduction of DFIG, AC/DC/AC converter control and finally the SIMULINK/MATLAB simulation for isolated Induction generator as well as for grid connected Doubly Fed Induction Generator and corresponding results and waveforms are displayed.

II. WIND ENERGY CONVERSION SYSTEM

Wind energy conversion system (WECS) is the overall system that converts the wind energy into useful electrical power through a mechanical power. The WECS consists of three major aspects aerodynamic, mechanical and electrical aspect. The major parts included in the mechanical and the electrical power conversion of a typical wind turbine system are shown in figure 1..

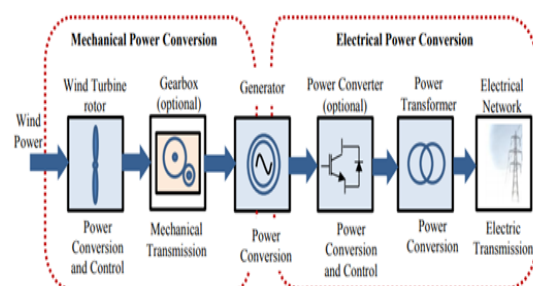


Figure 1: Block diagram showing the components of WECS connected to grid.

3. STEADY-STATE OPERATION OF THE DOUBLY-FED INDUCTION GENERATOR (DFIG)

The DFIG is an induction machine with a wound rotor where the rotor and stator are both connected to electrical sources, hence the term ‘doubly-fed’. The rotor has three phase windings which are energized with three-phase currents. These rotor currents establish the rotor magnetic field. The rotor magnetic field interacts with the stator magnetic field to develop torque. The magnitude of the torque depends on the strength of the two fields (the stator field and the rotor field) and the angular displacement between the two fields. Mathematically, the torque is the vector product of the stator and rotor fields. Conceptually, the torque is developed by magnetic attraction between magnet poles of opposite polarity where, in this case, each of the rotor and stator magnetic fields establish a pair of magnet poles, Figure 2. Clearly, optimum torque is developed when the two vectors are normal to each other. If the stator winding is fed from a 3-phase balanced source the stator flux will have a constant magnitude and will rotate at the synchronous speed. We will use the per-phase equivalent circuit of the induction machine to lay the foundations for the discussion of torque control in the DFIG. The equivalent circuit of the induction machine is shown in Figure 2.2. The stator side has two ‘parasitic’ components, R_s and L_s , which represent the resistance of the stator phase winding and the leakage inductance of the phase winding respectively. The leakage inductance models all the flux generated by current in the stator windings that does not cross the air-gap of the machine, it is therefore not useful for the production of torque. The stator resistance is a natural consequence of the windings being fabricated from materials that are good conductors but nonetheless have finite conductance (hence resistance). The magnetising branch, L_m , models the generation of useful flux in the machine – flux that crosses the air-gap either from stator to rotor or vice-versa.

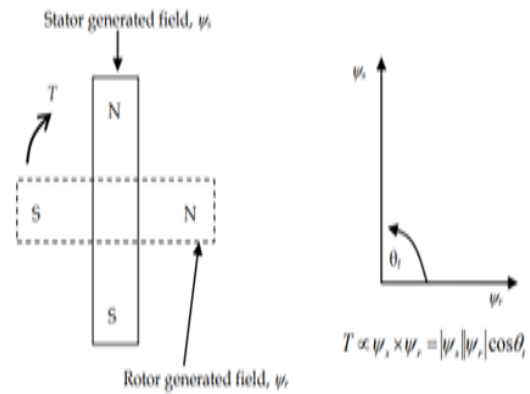


Figure 2: Magnetic pole system generated by currents in the stator and rotor windings. The stator and the rotor field generate a torque that tends to try and align poles of opposite polarity. In this case, of rotor experiences a clockwise torque.

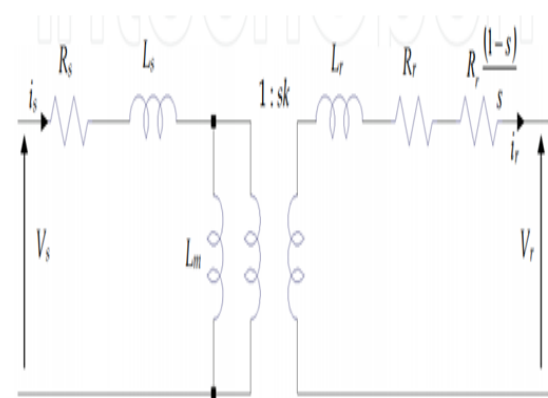


Figure 3: Per-phase equivalent circuit of an induction machine.

Like the stator circuit, the rotor circuit also has two parasitic elements. The rotor leakage reactance, L_r , and the rotor resistance R_r . In addition, the rotor circuit models the generated mechanical power by including an additional rotor resistance component, $R_r(1-s)/s$. Note that the rotor and stator circuits are linked via a transformer whose turns ratio depends on the actual turns ratio between the stator and rotor ($1:k$), and also the slip, s , of the machine. In an induction machine the slip

$$s = \frac{n_s - n_r}{n_s}$$

is defined as

where n_s and n_r are the synchronous speed and the mechanical speed of the rotor respectively. The synchronous speed is given

$$\text{by } n_s = \frac{60f_e}{p} \text{ rpm}$$

where p = number of pole pairs and f_e is the electrical frequency of the applied stator voltage. We will first consider the operation of the machine as a standard induction motor. If the rotor circuit is left open circuit and the rotor locked (standstill), when stator excitation is applied, a voltage will be generated at the output terminals of the rotor circuit, V_r . The frequency of this output will be at the applied stator frequency as slip in this case is 1. If the rotor is turned progressively faster and faster in the sub-synchronous mode, the frequency at the output terminals of the rotor will decrease as the rotor accelerates towards the synchronous speed. At synchronous speed the rotor frequency will be zero. As the rotor accelerates beyond synchronous speed (the super-synchronous mode) the frequency of the rotor voltage begins to increase again, but has the opposite phase sequence to the sub-synchronous mode. Hence, the frequency of the rotor voltage is

$$f_r = sf_e$$

No rotor currents can flow with the rotor open circuit; hence there is no torque production as there is no rotor field ψ_r , Figure 1. If the rotor was short circuited externally, rotor currents can flow, and they will flow at the frequency given by (2.3). The rotor currents produce a rotor magnetic field, ψ_r , which rotates at the same mechanical speed as the stator field, ψ_s . The two fields interact to produce torque, Figure 1. It is important to recognize that the rotor magnetic field and the stator magnetic field both rotate at the synchronous speed. The rotor may be turning asynchronously, but the rotor field rotates at the same speed as the stator field. The mechanical torque generated by the machine is found by calculating the power absorbed (or generated) by the rotor resistance component $R_r(1-s)/s$. This is shown to be

$$P_{mech} = 3|i_r'|^2 \left(\frac{1-s}{s}\right) R_r$$

In an ideal induction machine, we can ignore the rotor and stator phase winding resistance and leakage inductance. The per-

phase equivalent circuit then becomes simple, Figure 3. The phasor diagram for the machine is shown. Note that the stator generated flux component is normal to the rotor current (hence rotor flux) phasor giving the optimum conditions for

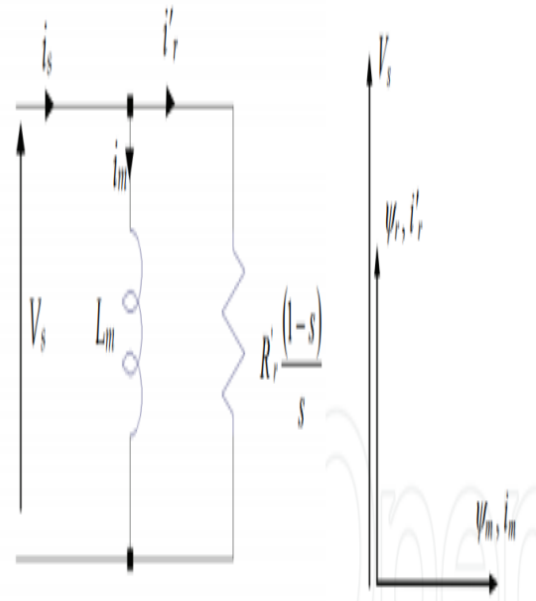


Figure 4: Simplified equivalent circuit of the induction machine assuming low values of slip and negligible stator and rotor leakage reactance. Phasor diagram demonstrates optimal orientation of magnetising current and rotor current.

Torque production (note this is true for low values of slip only). Using this simplified circuit diagram, the mechanical torque production is then:

$$T_{mech} = \frac{3|i_r'|^2 \left(\frac{1-s}{s}\right) (R_r')}{\omega_m}$$

As $\omega_m = \left(\frac{1-s}{p}\right) \omega_s$ and $\psi_m = L_m i_m' = \frac{V_s}{\omega_s} = \frac{|i_r'|}{s\omega_s} R_r'$

$$T_{mech} = 3|i_r'|^2 \left(\frac{1-s}{s}\right) \frac{R_r'}{\omega_m} = 3p \frac{|i_r'|}{s\omega_s} R_r' |i_r'| = 3p \psi_m |i_r'|$$

Another advantage of the DFIG technology is the ability for power electronic converters to generate or absorb reactive power, thus eliminating the need for installing capacitor banks as in the case of squirrel-cage induction generator.

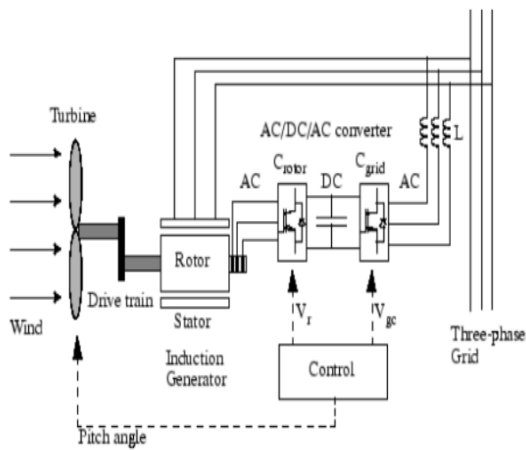


Figure 5: basic diagram of doubly fed induction generator with converters

Where V_r is the rotor voltage and V_g is grid side voltage. The AC/DC/AC converter is basically a PWM converter which uses sinusoidal PWM technique to reduce the harmonics present in the wind turbine driven DFIG system. Here C_{rotor} is rotor side converter and C_{grid} is grid side converter. To control the speed of wind turbine gear boxes or electronic control can be used.

4. OPERATING PRINCIPLE OF DFIG

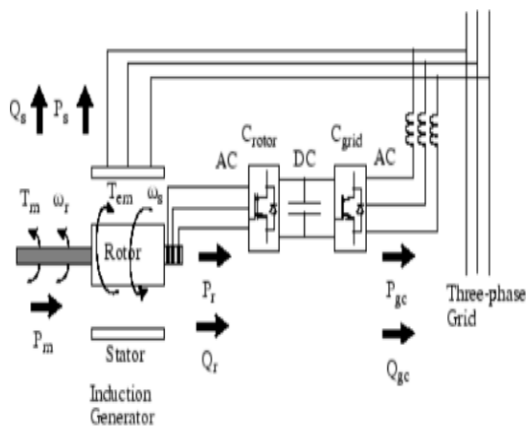


Figure 6: Power flow diagram of DFIG

The mechanical power and the stator electric power output are computed as follows:

$$P_r = T_m \cdot \omega_r \quad P_s = T_{em} \cdot \omega_s$$

For a loss less generator the mechanical equation is:

$$J \frac{d\omega_r}{dt} = T_m - T_{em}$$

In steady-state at fixed speed for a loss less generator $T_m = T_{em}$ and

$$P_m = P_s + P_r \text{ and It follows that:}$$

$$P_r = P_m - P_s = T_m \omega_r - T_{em} \omega_s$$

$$s = \frac{\omega_s - \omega_r}{\omega_s}$$

Where ω_s is defined as the slip of the generator

Generally the absolute value of slip is much lower than 1 and, consequently, P_r is only a fraction of P_s . Since T_m is positive for power generation and since ω_s is positive and constant for a constant frequency grid voltage, the sign of P_r is a function of the slip sign. P_r is positive for negative slip (speed greater than synchronous speed) and it is negative for positive slip (speed lower than synchronous speed). For super synchronous speed operation, P_r is transmitted to DC bus capacitor and tends to rise the DC voltage. For sub-synchronous speed operation, P_r is taken out of DC bus capacitor and tends to decrease the DC voltage. C_{grid} is used to generate or absorb the power P_{gc} in order to keep the DC voltage constant. In steady-state for a lossless AC/DC/AC converter P_{gc} is equal to P_r and the speed of the wind turbine is determined by the power P_r absorbed or generated by C_{rotor} . The phase-sequence of the AC voltage generated by C_{rotor} is positive for sub-synchronous speed and negative for super synchronous speed. The frequency of this voltage is equal to the product of the grid frequency and the absolute value of the slip. C_{rotor} and C_{grid} have the capability for generating or absorbing reactive power and could be used to control the reactive power or the voltage at the grid terminals.

5. DYNAMIC SIMULATION OF DFIG IN TERMS OF D-Q WINDING

The general model for wound rotor induction machine is similar to any fixed-speed induction

Generator as follows:

1. Voltage equations:
Stator Voltage Equations:

$$v_{qs} = p\lambda_{qs} + \omega\lambda_{qs} + r_s i_{qs}$$

Rotor Voltage Equations:

$$v_{qr} = p\lambda_{qr} + (\omega - \omega_r)\lambda_{dr} + r_r i_{qr}$$

2. Power Equations:

$$P_s = \frac{3}{2}(v_{ds} i_{ds} + v_{qs} i_{qs})$$

$$Q_s = \frac{3}{2}(v_{qs} i_{ds} - v_{ds} i_{qs})$$

3. Torque Equation

$$T_s = \frac{3p}{4}(\lambda_{qs} i_{ds} - \lambda_{ds} i_{qs})$$

4. Flux Linkage Equations:

Stator Flux Equations:

$$\lambda_{qs} = (L_{ls} + L_{rn})i_{qs} + L_m i_{qr}$$

Rotor Flux Equations:

$$\lambda_{qr} = (L_{lr} + L_{rn})i_{qr} + L_m i_{qs}$$

6. RESULT AND DISCUSSION

Turbine response to a change in wind speed

In the “Wind Speed” step block specifying the wind speed. Initially, wind speed is set at 8 m/s, then at $t = 5$ s, wind speed increases suddenly at 14 m/s. Start simulation and observe the signals on the “Wind Turbine” scope monitoring the wind turbine voltage, current, generated active and Reactive powers, DC bus voltage and turbine speed.

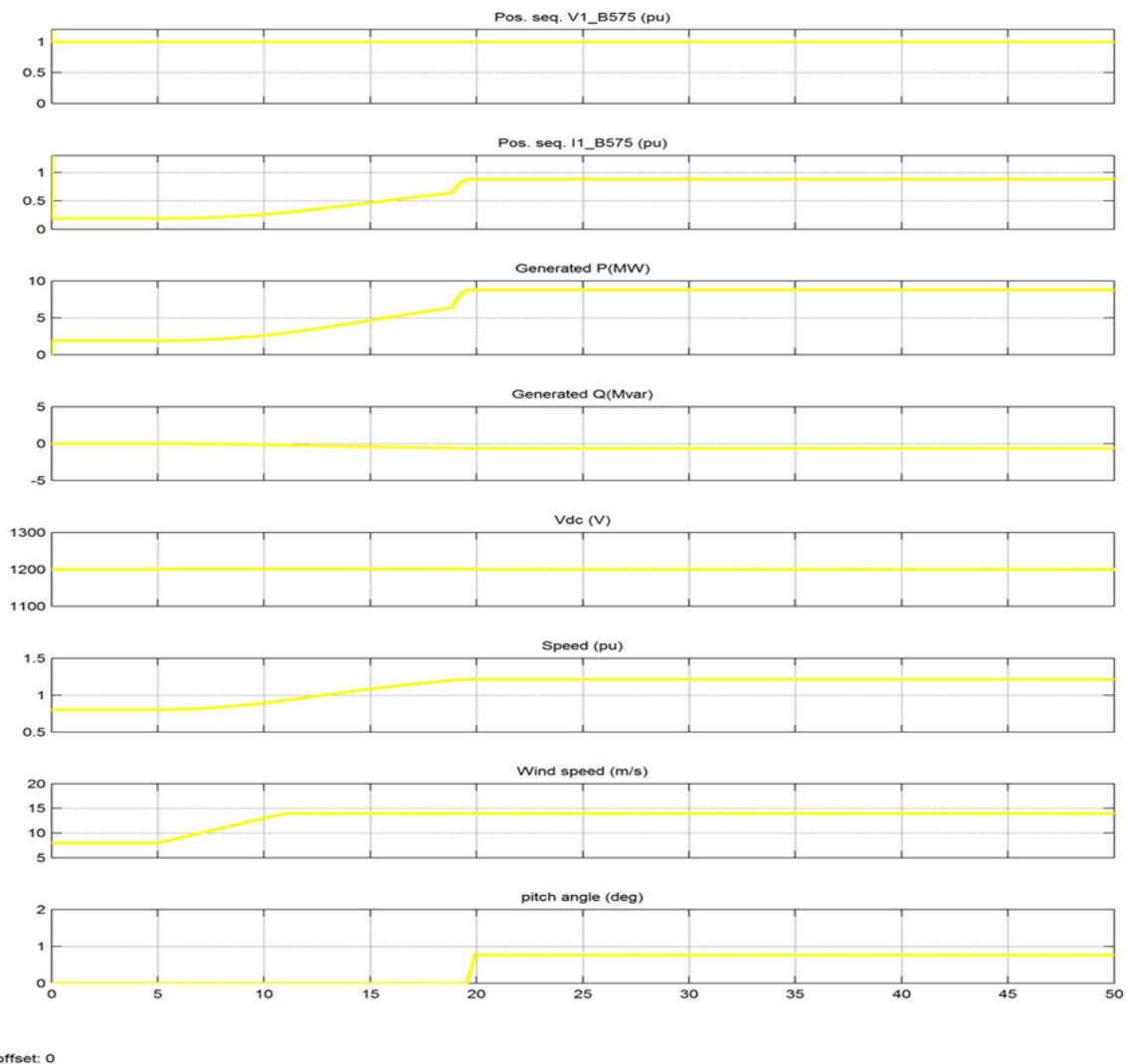


Figure 7: wind turbine voltages, current, generated active and Reactive powers, DC bus voltage and turbine speed

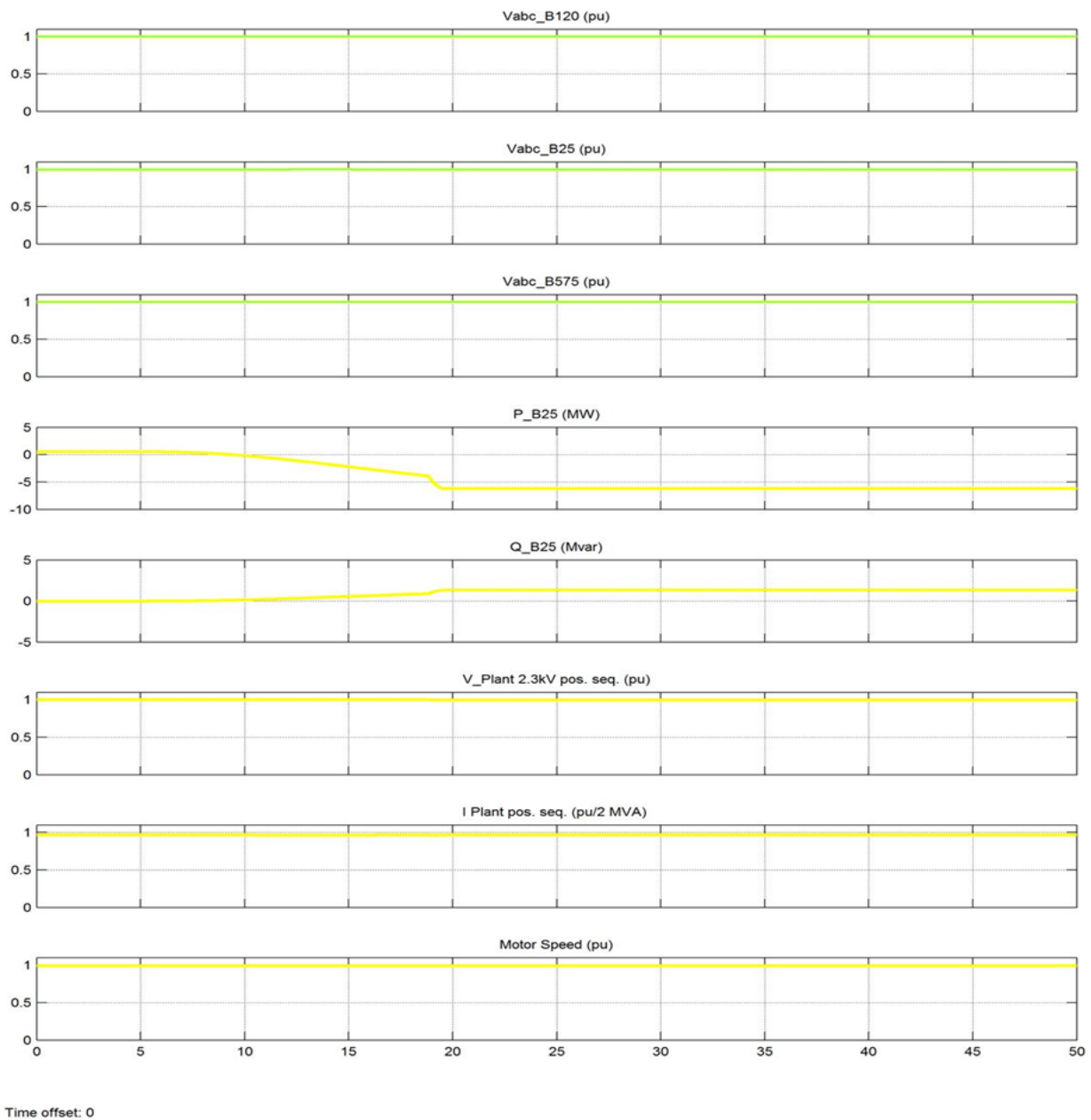


Figure 8: Bus voltage, current, generated active power, motor speed

At $t = 5$ s, the generated active power starts increasing smoothly (together with the turbine speed) to reach its rated value of 9 MW in approximately 20 s. Over that time frame the turbine speed will have increased from 0.8 PU to 1.21 PU. Initially, the pitch angle of the turbine blades is zero degree and the turbine operating point follows the red curve of the turbine power characteristics up to point D. Then the pitch angle is increased from 0 deg to 0.76 deg in order to limit the mechanical power. We also observed the

voltage and the generated reactive power. The reactive power is controlled to maintain a 1 PU voltage. At nominal power, the wind turbine absorbs 0.68 Mvar (generated $Q = -0.68$ Mvar) to control voltage at 1PU.

If we change the mode of operation to “Var regulation” with the “Generated reactive power Q_{ref} ” set to zero, we will observe that voltage increases to 1.021 PU when the wind turbine generates its nominal power at unity power factor.

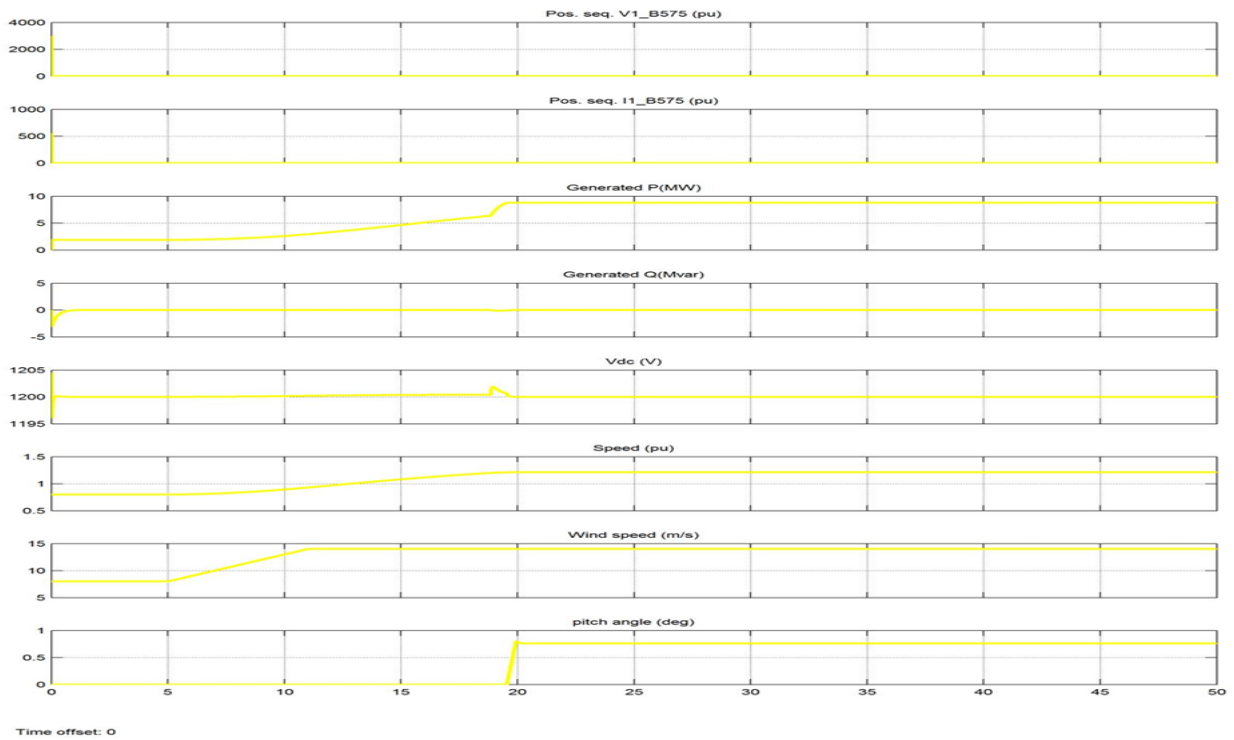


Figure 9: At Var regulation wind turbine voltage, current, generated active and Reactive powers, DC bus voltage and turbine speed

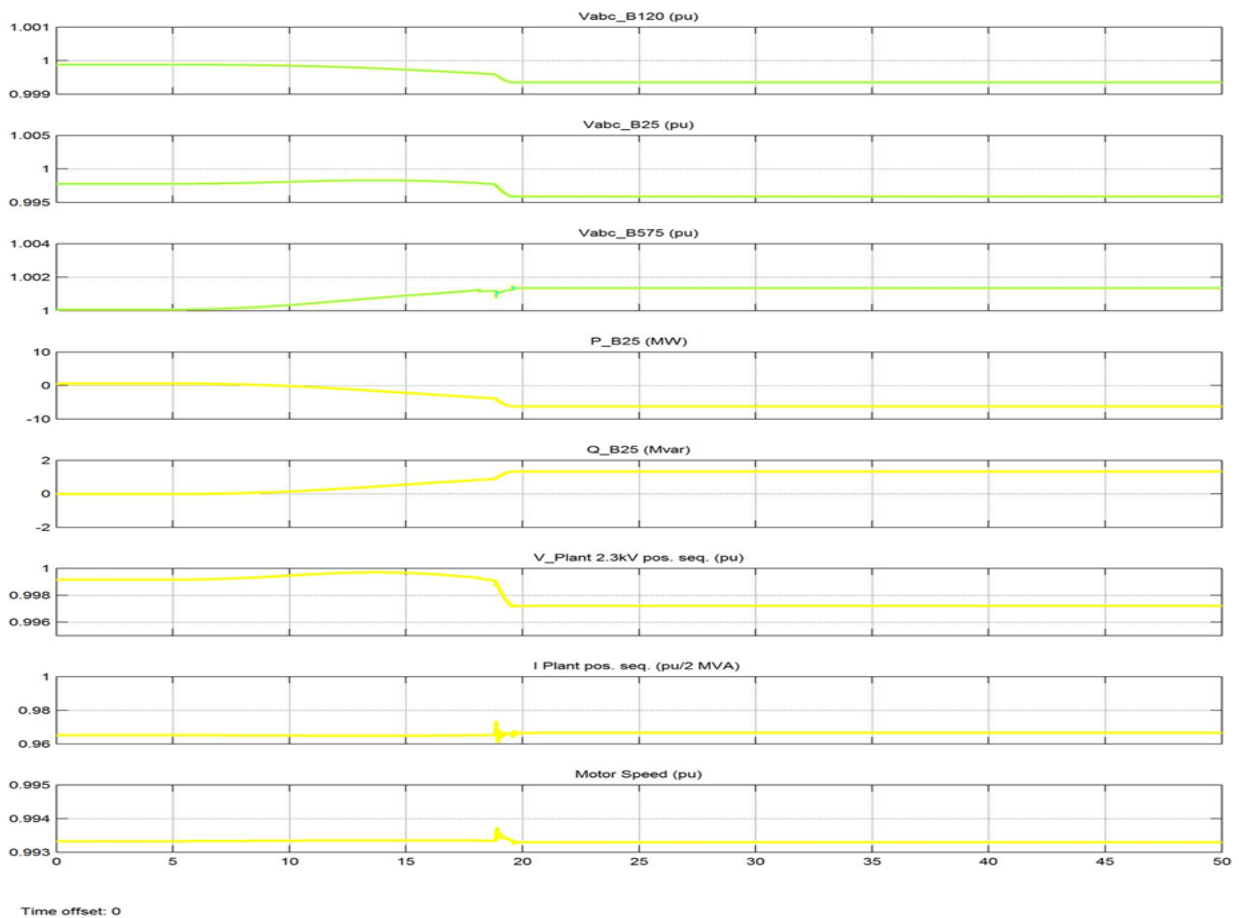


Figure 10: At Var regulation Bus voltage, current, generated active motor speed

In this mode the wind turbine speed varies very much starting from 0.7 PU to 1.6 PU and then tending to stabilize at 1.0 PU. At about $t = 12$ s the pitch angle increases abruptly.

Simulation of wind turbine and grid parameters when the mode of operation is set to Control Parameters

When the mode of operation is set to control parameters then we see that for grid the active power starts decreasing after 5 s and becomes nearly 5 MW while the reactive power becomes positive and starts increasing to nearly 2MW before becoming constant.

In the grid side simulation the active power generated starts increasing as the voltage increases and reaches to nearly 9 MW as the voltage reaches to 1 Pu. The reactive power requirement is less initially but gradually it increases to few MWs. The wind turbine speed remains constant for 7 s then it increases and again becomes constant at 20 s. In this observe the impact of voltage sag

resulting from a remote fault on the 120-kV system. First, in the wind speed step block, disable the wind speed step by changing the Final value from 14 to 8 m/s. Then open the 120-kV voltage source menu. In the parameter “Time variation of”, select “Amplitude”. A 0.15 pu voltage drop lasting 0.5 s is programmed to occur at $t = 5$ s. Make sure that the control mode is still in Var regulation with $Q_{ref} = 0$. Start simulation and open the “Grid” scope. Observe the plant voltage and current as well as the motor speed. Note that the wind farm produces 1.87 MW. At $t = 5$ s, the voltage falls below 0.9 pu and at $t = 5.22$ s, the protection system trips the plant because an under voltage lasting more than 0.2 s has been detected (look at the protection settings and status in the “Plant” subsystem). The plant current falls to zero and motor speed decreases gradually, while the wind farm continues generating at a power level of 1.87 MW. After the plant has tripped, 1.25 MW of power (P_{B25} measured at bus B25) s exported to the grid.

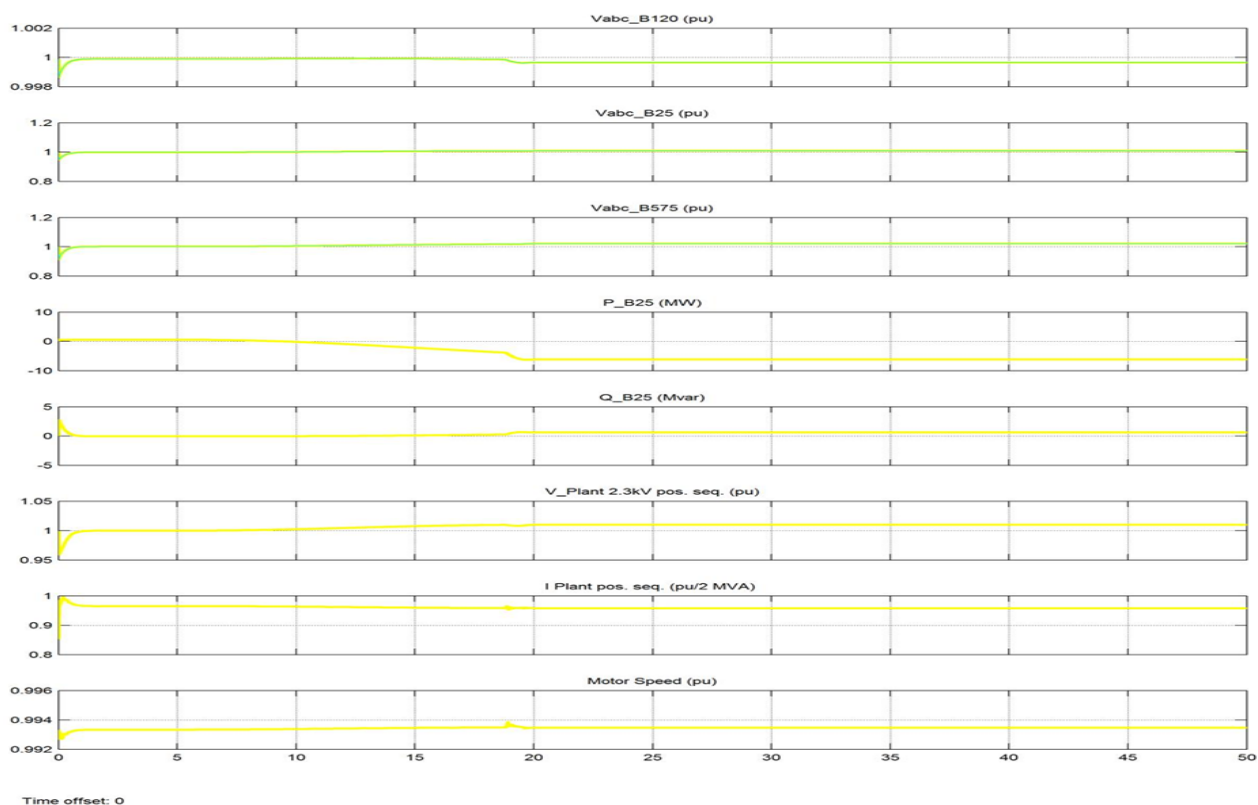


Figure 11: At Control Parameters Bus voltage, current, generated active motor speed

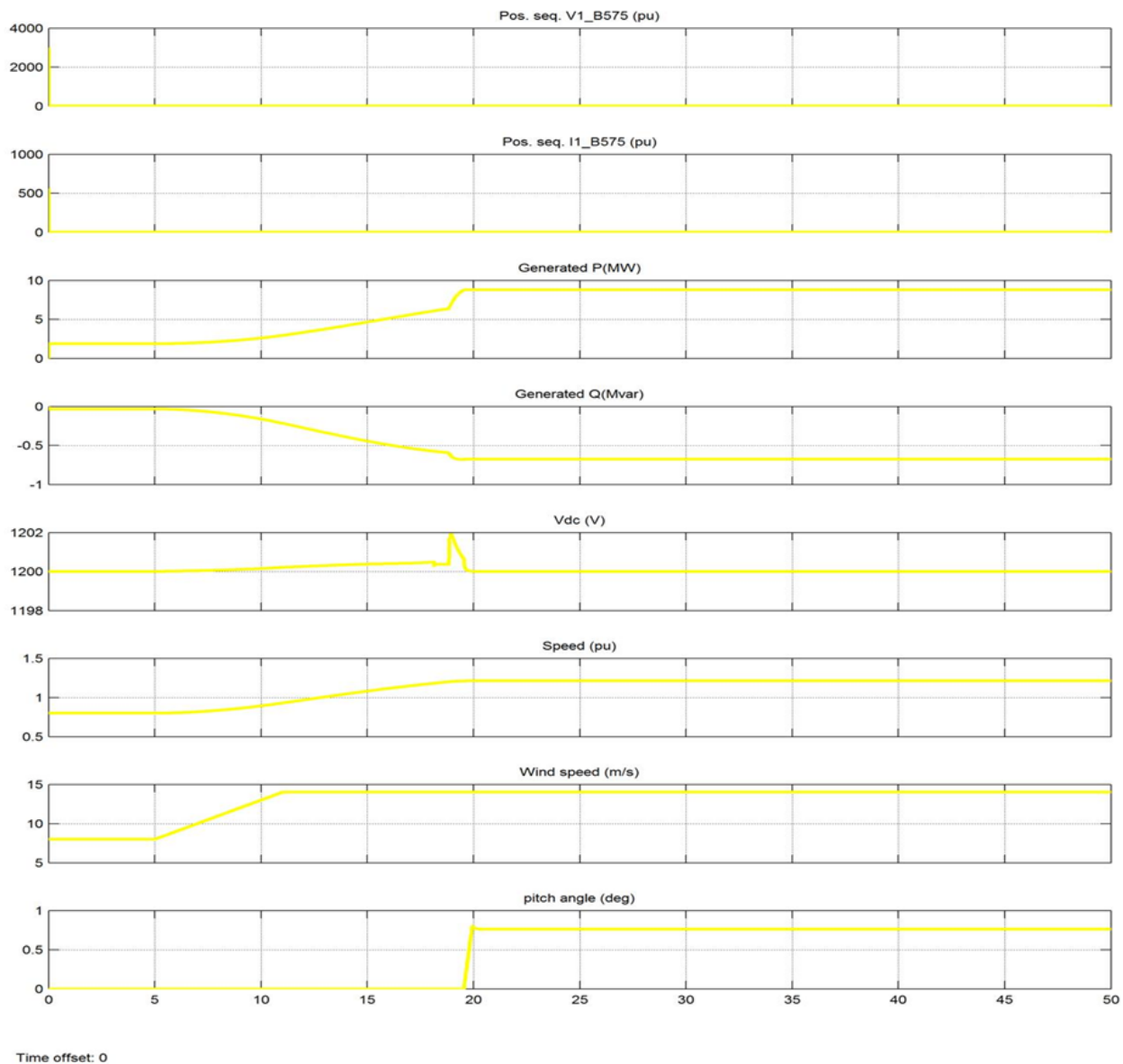


Figure 12: Simulation of a voltage sag on the 120-kV system

Now, we changed the wind turbine control mode to “Voltage regulation” and repeat the test. We will notice that the plant does not trip anymore. This is because the voltage support provided by the 5 Mvar reactive powers generated by the wind-turbines during the voltage sag keeps the plant Voltage above the 0.9 pu protection threshold. The plant voltage during the voltage sag is now 0.93 pu. Finally, we will now observe impact of a single phase-to-ground fault occurring on the 25-kV line at B25 bus. First disable the 120-kV voltage step. Now open the “Fault” block menu and select “Phase A Fault”. Check that the fault is programmed to

apply a 9-cycle single-phase to ground fault at $t = 5$ s. We observed that when the wind turbine is in “Voltage regulation” mode, the positive-sequence voltage at wind-turbine terminals (V1_B575) drops to 0.8 pu during the fault, which is above the under voltage protection threshold (0.75 pu for a $t > 0.1$ s). The wind farm therefore stays in However, if the “Var regulation” mode is used with $Q_{ref} = 0$, the voltage drops under 0.7 pu and the under voltage protection trips the wind farm. We can now observe that the turbine speed increases. At $t = 40$ s the pitch angle starts to increase in order to limit the speed.

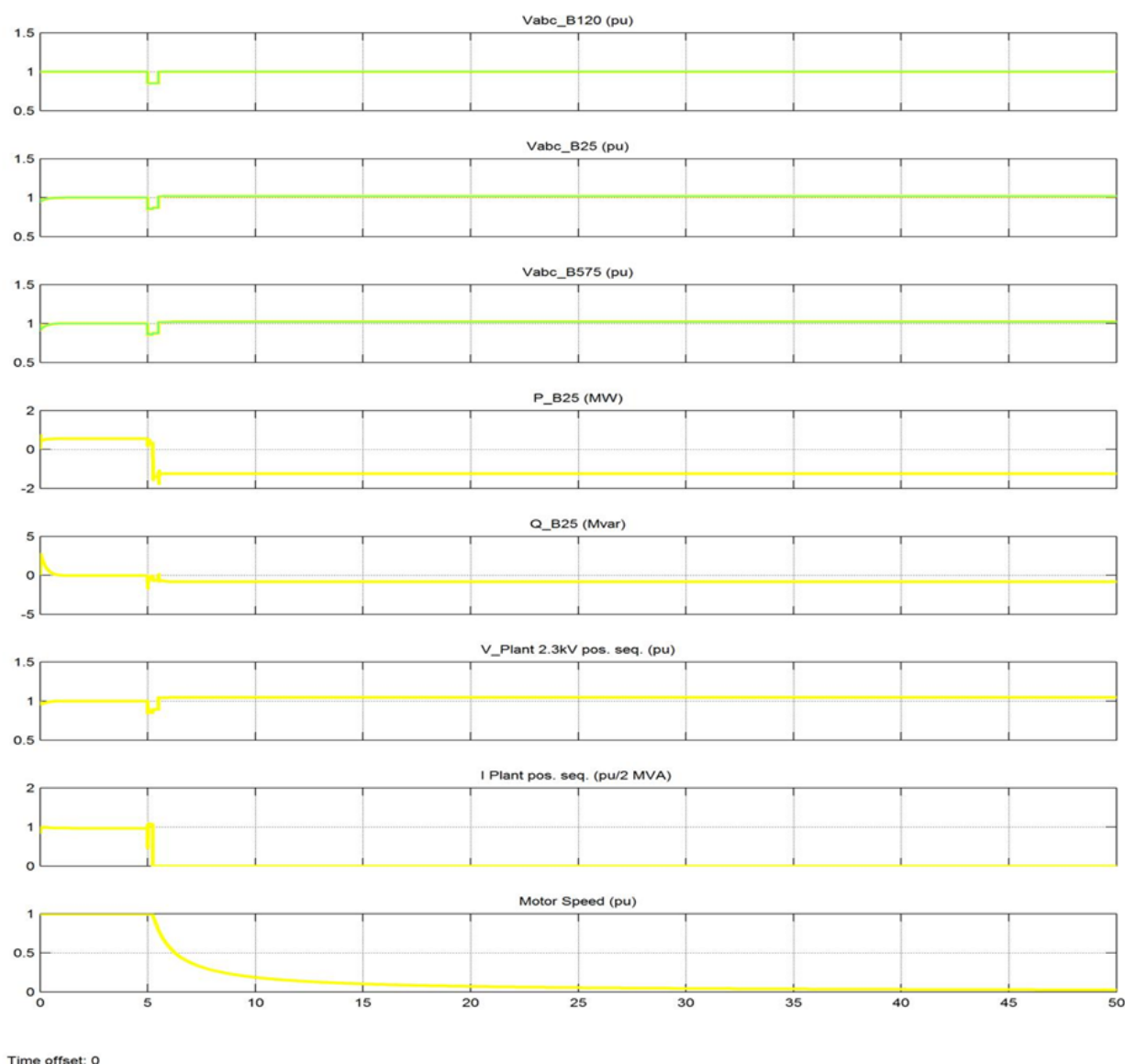


Figure 13: Simulation of a fault on the 25-kV system

7. CONCLUSION

We have discussed here the basic operation of DFIG and its controls using AC/DC/AC converter. First we simulated a wind turbine driven isolated (not connected to grid) induction generator. But for best efficiency the DFIG system is used which is connected to grid side and has better control. The rotor side converter (RSC) usually provides active and reactive power control of the machine while the grid-side converter (GSC) keeps the voltage of the DC-link constant. So finally we simulated grid side and wind turbine side parameters and the corresponding results have been displayed. The model is a discrete-time

version of the Wind Turbine Doubly-Fed Induction Generator (Pharos Type) of Matlab/SimPower Systems. Here we also took the protection system in consideration which gives a trip signal to the system when there is a fault (single phase to ground fault) on the system. The faults can occur when wind speed decreases to a low value or it has persistent fluctuations. The DFIG is able to provide a considerable contribution to grid voltage support during short circuit periods. Considering the results it can be said that doubly fed induction generator proved to be more reliable and stable system when connected to grid side with the proper converter control systems.

REFERENCES:

- [1] Hans Øverseth Røstøen Tore M. Undeland Terje Gjengedal' IEEE paper on doubly fed induction generator in a wind turbine.
- [2] S. K Salman and Babak Badrzadeh "School of Engineering", The Robert Gordon University, IEEE paper on New Approach for modelling Doubly-Fed Induction Generator (DFIG) for grid-connection studies.
- [3] Sloomweg JG, Polinder H, Kling WL. "Dynamic modeling of a wind turbine with doubly fed induction generator". IEEE Power Engineering summer meeting, 2001; Vancouver, Canada.
- [4] Holdsworth L, Wu XG, Ekanayake JB, Jenkins N. "Comparison of fixed speed and doubly-fed induction wind turbines during power system disturbances". IEE Proceedings: Generation, Transmission, Distribution, 2003, 3: 343-352
- [5] Ekanayake, J.B, Holdsworth, L, Wu, X., Jenkins, N. "Dynamic modeling of Doubly Fed Induction generator wind turbines". IEEE Transaction on Power Systems, 2003, 2:803-809
- [6] J. Morren, J.T.G. Pierik, S.W.H. de Haan, J. Bozelie, "Grid interaction of offshore wind farms. Part 1. Models for dynamic simulation", Wind Energy, 8 (3): JUL-SEP 2005.
- [7] R. Pena, J.C. Clare, G.M. Asher, "Doubly-fed induction generator using back-to-back PWM converters and its applications to variable-speed wind-energy generation, "IEEE Proceedings on Electrical Power Applications", Vol. 143, No. 3, May 1996, pp. 231-341.
- [8] The MathWorks, "SimPowerSystems For Use with Simulink", User's Guide Version
- [9] Richard Gagnon, Gilbert Sybille, Serge Bernard, Daniel Paré, Silvano Casoria, Christian Larose "Modeling and Real-Time Simulation of a Doubly-Fed Induction Generator-Driven by a Wind Turbine" Presented at the International Conference on Power Systems Transients (IPST'05) in Montreal, Canada on June 19-23, 2005 Paper No. IPST05-162.